Parity nonconservation for neutron resonances in ^{238}U

X. Zhu,[1],* J. D. Bowman,[2] C. D. Bowman,[2] J. E. Bush,[3],† P. P. J. Delheij,[4] C. M. Frankle,[3],‡
C. R. Gould,[3] D. G. Haase,[3] J. N. Knudson,[2] G. E. Mitchell,[3] S. Penttilä,[2] H. Postma,[5] N. R. Roberson,[1]
S. J. Seestrom,[2] J. J. Szymanski,[2],§ and V. W. Yuan[2]

(TRIPLE Collaboration)

[1]Duke University, Durham, North Carolina 27706
and Triangle Universities Nuclear Laboratory, Durham, North Carolina 27706
[2]Los Alamos National Laboratory, Los Alamos, New Mexico 87545
[3]North Carolina State University, Raleigh, North Carolina 27695
and Triangle Universities Nuclear Laboratory, Durham, North Carolina 27706
[4]TRIUMF, Vancouver, British Columbia, Canada V6T 2A3
[5]University of Technology, P.O. Box 5046, 2600 GA, Delft, The Netherlands
(Received 6 April 1992)

Parity nonconservation (PNC) was studied for 16 p-wave resonances in ^{238}U by measuring the helicity dependence of the total cross section for epithermal neutrons scattered from ^{238}U. A statistical analysis yields a root-mean-square PNC matrix element $M = 0.56^{+0.41}_{-0.20}$ meV, which corresponds to a spreading width of $\Gamma^{\mathrm{PV}} = 0.9 \times 10^{-7}$ eV. Under plausible assumptions this gives a value of 4×10^{-7} for $|\alpha_p|$, the ratio of strengths of the P-odd and P-even effective nucleon-nucleon interactions.

I. INTRODUCTION

There have been extensive experimental and theoretical efforts on parity nonconservation (PNC) effects in light nuclei. A recent review summarizes the status in light nuclei [1]. Here we focus on PNC effects in neutron-nucleus interactions in heavy nuclei.

Parity violation in the neutron-nucleus interaction was first observed by Abov et al. [2] with a polarized neutron beam and an unpolarized target. These experimental results were later confirmed a number of times [3–6]. A comprehensive review of the early work with polarized neutron beams is given by Krupchitsky [7].

Michel [8] suggested that the forward scattering amplitude would have a PNC component due to the weak interaction. There are two convenient PNC observables which arise from polarized neutron transmission through a target—spin rotation (of the neutron polarization vector about its momentum) and helicity dependence of the total cross section—corresponding to the real and imaginary parts of the scattering amplitude [9]. Forte et al. [10] performed a neutron polarizer-analyzer experiment similar to an optical polarizer-analyzer experiment. Us-

ing cold neutrons from the Grenoble high flux reactor and an identical polarizer and analyzer, they observed parity violation in ^{117}Sn. Subsequently Heckel et al. [11] observed neutron spin rotation in a number of nuclei.

In all of these measurements the parity violations were large compared to the expected scale of 10^{-7}, but were still small on an absolute scale. Sushkov and Flambaum [12,13] suggested that the mechanism of compound nuclear mixing between close-lying states with the same total angular momentum J but opposite parity π could lead to very large parity violations. Alfimenkov et al. [14] observed an extremely large parity violation (7.3±0.5%) at the 0.73-eV resonance in ^{139}La. This effect has since been confirmed at IAE [15] (7.6±0.6%), KEK [16] (9.7±0.5%), Los Alamos [17] (9.2±1.7%), and recently again at Los Alamos [18] (10.15±0.45% and 9.55±0.35%) by our group. The last measurement used La as both polarizer and target. Since this "double lanthanum" measurement does not require a separate determination of the polarization of the neutron beam, we consider the value of 9.55% obtained with this method to be the most reliable of all of the measurements of the parity violation for the 0.73 eV resonance in ^{139}La. We now use this value (9.55%) for calibration purposes to determine the neutron polarization [18].

Parity violation also was observed in ^{81}Br, ^{111}Cd, and ^{117}Sn by Alfimenkov et al. [14]. The limitation in these experiments is the observation of only one parity violation per nuclide. We decided to utilize the intense neutron beam at the Los Alamos Neutron Scattering Center (LANSCE) to study parity violation. The experimental goal was to study parity violation for many resonances in a single nucleus. Preliminary reports on our first PNC experiments have been published for ^{238}U [19] and ^{232}Th

[20]. Here we present the final results for ^{238}U. The following paper [21] presents our results for ^{232}Th.

We define the parity-violating asymmetry P for an $l=1$ (p-wave) resonance from

$$\sigma^{\pm}=\sigma_p(1\pm f_nP) ,\qquad (1)$$

where $\sigma^{\pm}$ is the resonance cross section for $+$ and $-$ helicity neutrons, σ_p the resonance part of the p-wave cross section, and f_n the neutron polarization. The simplest explanation for the parity violation is that the p-wave resonance mixes with neighboring s-wave resonances with the same angular momentum J. Here we consider only mixing with one s-wave resonance—the two-level approximation. This simple approximation conveniently illustrates most of the physics. In Sec. V we remove this restriction and explicitly include the effects of many s-wave resonances. The effect of distant states is now under active consideration: this issue is discussed in the following paper.

For a target with spin $I=0$, the total angular momentum is $J=l+s$, where l and s are the neutron orbital angular momentum and spin. For an s-wave resonance ($l=0$) $J=\frac{1}{2}$, while for a p-wave resonance ($l=1$) $J=\frac{1}{2}$ or $\frac{3}{2}$. Only the $J=\frac{1}{2}$ p-wave resonances can mix with the s-wave resonances and show parity nonconservation.

The nuclear Hamiltonian can be written $H=H_0+H_w$, where H_0 is the parity-conserving Hamiltonian and H_w is the small parity-violating part. The parity-violating term mixes the s and p resonances. If Ψ_s and Ψ_p are the unperturbed wave functions, then in first-order perturbation theory the wave functions of the mixed states are

$$\Psi'_s=\Psi_s+[V_{sp}/(E_s-E_p)]\Psi_p ,$$
$$\Psi'_p=-[V_{sp}/(E_s-E_p)]\Psi_s+\Psi_p ,\qquad (2)$$

where $V_{sp}=\langle\Psi_s|H_w|\Psi_p\rangle$, and E_s and E_p are the energies of the s- and p-wave resonances. We assume time-reversal invariance holds. The matrix element V_{sp} is then pure real or pure imaginary depending on the phase convention adopted for the wave function Ψ. For scattering problems, the convention $T\Psi(J,M)\to(-1)^{J-M}\Psi(J,-M)$ is usually adopted, and V_{sp} is real. [For bound state problems the Condon and Shortley phase convention is usually adopted: $T\Psi(J,J)\to(-1)^{2M}\Psi(J,-M)$, and V_{sp} is pure imaginary [22].] In the present work we follow the convention for scattering and take V_{sp} real. The parity-violating asymmetry has been obtained by many authors [12,23–26]. The p-wave cross section can be written as

$$\sigma^{\pm}=\sigma_p\pm f_n\sigma_{\rm PNC} .\qquad (3)$$

Clearly $P=\sigma_{\rm PNC}/\sigma_p$. For a spin-zero target $\sigma_{\rm PNC}$ is

$$\sigma_{\rm PNC}=2\pi\lambda^2V_{sp}(\Gamma_s^n\Gamma_p^n)^{1/2}\frac{[\Delta E_s\Gamma_p+\Delta E_p\Gamma_s]}{[S]^2[P]^2} ,\qquad (4)$$

where $\Delta E_s=E_s-E$ and $[S]^2=\Delta E_s^2+\Gamma_s^2/4$, and similarly for the p-wave resonance. E is the kinetic energy of the neutron-nucleus pair in the center-of-mass system, Γ_s^n and Γ_p^n are the neutron partial widths, Γ_s and Γ_p are the total widths, and λ is the de Broglie wavelength in the

c.m. system. In this notation, $\sigma_p=\pi\lambda^2\Gamma_p^n\Gamma_p/[P]^2$. At the p-wave resonance $E=E_p$ and $\Delta E_p=0$. We also assume that the p-wave widths (typically ~ 20 meV in ^{238}U) are much smaller than the level spacing (~ 10 eV in ^{238}U). Then P becomes approximately

$$P\approx[2V_{sp}/(E_s-E_p)][\Gamma_s^n(E_p)/\Gamma_p^n(E_p)]^{1/2} .\qquad (5)$$

The energy dependence of the s-wave neutron width is $\Gamma_s^n(E)=\Gamma_s^n(E_s)(E/|E_s|)^{1/2}$. The parity-violating cross section $\sigma_{\rm PNC}$ at the peak of the s-wave resonance is about the same as at the peak of the p-wave resonance, but the s-wave cross section is orders of magnitude larger than the p-wave cross section. Therefore the parity-violating asymmetry, i.e., the ratio $\sigma_{\rm PNC}/\sigma_s$, is much smaller than the corresponding ratio $\sigma_{\rm PNC}/\sigma_p$.

The ratio $V_{sp}/(E_s-E_p)$ is usually called dynamic enhancement. This has been discussed by many authors, including Sushkov [13], Bunakov [27], Desplanques [28], and Weidenmüller [29]. The key qualitative conclusion is that the complicated compound nuclear (CN) system, this ratio is enhanced by a factor of $N^{1/2}$ relative to the value in the nucleon-nucleon system, where N is the number of components in the compound nuclear wave function. Since N is approximately $\Delta E/D$, where ΔE is the scale of the strong interaction (~ 1 MeV) and D is the average level spacing (~ 10 eV), N is of order 10^5, and the dynamical enhancement is about 3×10^2.

The ratio $[\Gamma_s^n(E_p)/\Gamma_p^n(E_p)]^{1/2}$ is usually called kinematic enhancement. The neutron width $\Gamma_s^n\sim kR$ and $\Gamma_p^n\sim(kR)^3$, where k is the neutron wave number and R is the radius of the ^{238}U nucleus. For a 1 eV neutron $k\sim 2.2\times 10^{-4}$ fm^{-1}, $R\sim 10$ fm, and the kinematic enhancement factor is about 5×10^2. Therefore the combination of dynamic and kinematic enhancement is of order 10^5. Since PNC effects are about 10^{-7} in the nucleon-nucleon (NN) system, this 10^5 enhancement factor makes physically plausible PNC asymmetries in the compound nuclear (CN) system of order 1%.

If the resonance parameters are known, then (in the two-level approximation) the PNC matrix element V_{sp} can be determined. The parity violation arises from the mixing of two very complicated states. In fact, the compound nucleus is considered a chaotic system [30]. Therefore each value of V_{sp} is a matrix element sampled at random from the distribution of PNC matrix elements. There is a clear analogy with ordinary nuclear transition matrix elements. One nuclear reduced width has little information content. The information is contained in the ensemble of reduced widths, the Porter-Thomas distribution. Here the information content is in the distribution of PNC matrix elements. We assume that the PNC matrix elements are random variables, with a distribution with zero mean and variance M^2. The goal of the experiment is to determine this variance and therefore the root-mean-square PNC matrix element M.

The theoretical issue is to connect M with the properties of the NN interaction. It is convenient to introduce a parity-violating spreading width $\Gamma^{PV}=2\pi M^2/D$. Since M^2 is expected to be proportional to the level spacing, the spreading width should to be approximately independent of mass number.

Using the methods of statistical nuclear spectroscopy, French *et al.* [31,32] established a connection between symmetry breaking in the *CN* system and symmetry breaking in the effective *NN* system for time-reversal-invariance (TRI) violation. They obtained

$$\Gamma^{\text{TRIV}} = 2\pi \times 10^5 (\text{eV}) \alpha_T^2 , \qquad (6)$$

where Γ^{TRIV} is the TRI violating spreading width, and α_T is the ratio of the TRI violating strength to the TRI conserving strength in the effective *NN* interaction. We assume that the parity-violating spreading width is related to an α_p which is the ratio of the parity-violating strength to the parity-conserving strength

$$\Gamma^{\text{PV}} = 2\pi \times 10^5 (\text{eV}) \alpha_p^2 . \qquad (7)$$

Johnson *et al.* [33] have extended these ideas and established a connection with the mesonic coupling constants used to parametrize the parity-violation problem in light nuclei. Here we use this first approximation to provide a qualitative interpretation of the value of *M* extracted from our data.

The experimental method is described in Sec. II. The procedure to determine the longitudinal asymmetry from the data is discussed in Sec. III. The experimental data and the data reduction are presented in Secs. IV and V. These results are then analyzed in Sec. VI. A brief summary is given in Sec. VII.

II. EXPERIMENTAL METHOD

The details of the experimental procedure are given in Roberson *et al.* [34]. Here we provide only a brief description.

The 800-MeV proton beam from the Los Alamos Meson Physics Facility (LAMPF) linac is injected into a proton storage ring (PSR) where the beam is compressed from a pulse width of ~ 800 μs to a width of ~ 250 ns. The extracted proton beam strikes a tungsten target and neutrons (~ 20 per incident proton) are produced by the spallation process. The neutrons are moderated by water and collimated to produce a beam. Typical proton beam currents for the U experiment were ~ 50 μA. The beam is polarized by selective attenuation through a cell of longitudinally polarized protons. The protons are polarized with dynamic nuclear polarization at 1-K temperature and 2-T magnetic field. The 2-T magnetic field is either parallel or antiparallel to the beam direction. The absolute polarization was determined by measuring the transmission through the cell as a function of temperature. (Yuan *et al.* [18] discuss other methods of determining the absolute polarization of the neutron beam. For the ^{232}Th experiment [21] the "double lanthanum" method was used to obtain the absolute polarization.) The relative polarization of the beam is measured for each run by determining the proton polarization in the spin filter with NMR [34]. For the ^{238}U experiment the neutron polarization was about 45%.

Fast spin reversal was accomplished with a magnetic spin flipper [35]. In one configuration there is only a fixed longitudinal field which reverses sign at the midpoint of the spin flipper. A longitudinally polarized neutron passes through the transverse field region and does not reverse spin direction. To flip the neutron spin a transverse field is added to the longitudinal field. The spin then adiabatically follows the total magnetic field direction and reverses direction. The spin can be reversed using either direction of the transverse field. The spin-preserving efficiency and the spin-flipping efficiency are discussed in Sec. V. We implement a transverse field sequence $\{0, +, -, 0, +, 0, 0, -\}$ which produces a spin-state sequence $\{$parallel, antiparallel, $A, P, A, P, P, A \}$ (or vice versa). This sequence eliminates in first order the effect of transverse stray fields on the system and linear and quadratic time drifts in the detectors. The spin direction was reversed every ten seconds. The direction of polarization of the protons in the spin filter also can be reversed by changing the microwave pumping frequency without changing the magnetic field.

The polarized neutrons passed through a target located at the beam exit of the spin flipper. The ^{238}U target was a metallic sample of thickness 0.091 atom/b in the shape of a cylinder of diameter 5.1 cm and length 1.91 cm. The target was depleted to 0.2% of ^{235}U. The neutrons were detected by ^{6}Li-loaded glass detectors located at 56 m from the neutron source. The count rates were so high that there was a high probability of neutron pulses overlapping. Instead of counting each neutron pulse individually, we employed a current mode technique. The details are given by Bowman *et al.* [36].

The neutron beam was monitored with a thin ^{6}Li glass paddle detector placed directly in front of the biological shield. At the end of each eight-step sequence the average value of the neutron flux is determined; if the average flux is outside a predetermined value that data is routed to a separate "bad" data area. Each spin state was held for 200 neutron bursts (10 s) and the eight-step spin-state sequence was completed in about 90 s. This sequence was repeated for 20 times and these data combined into a "run." The process was then repeated several times.

III. DETERMINATION OF LONGITUDINAL ASYMMETRIES

The total cross section for a *p*-wave resonance is

$$\sigma = \sigma_{\text{pot}} + \sigma^{\pm} = \sigma_{\text{pot}} + \sigma_p (1 \pm f_n P) , \qquad (8)$$

where σ_{pot} is the potential scattering cross section. The neutron transmission yield at the detector is given by

$$N^{\pm} = F(E_n) \exp\{ -nt[\sigma_{\text{pot}} + \sigma_p (1 \pm f_n P)] \}$$
$$= C(E_n) \exp[-nt\sigma_p (1 \pm f_n P)] , \qquad (9)$$

where $F(E_n)$ is the neutron flux, E_n the neutron energy, $C(E_n) = F(E_n) \exp[-nt\sigma_{\text{pot}}]$, *n* is the number density of the ^{238}U target nuclei, and *t* is the thickness of the target. The transmission asymmetry ε is defined as

$$\varepsilon = (N^+ - N^-)/(N^+ + N^-) = -\tanh(n\sigma_p t f_n P) . \qquad (10)$$

If the argument is small, then $\varepsilon \approx -n\sigma_p t f_n P$.

The transmission yield and the asymmetry are shown in Fig. 1 for the 63.5-eV *p*-wave resonance. This reso-
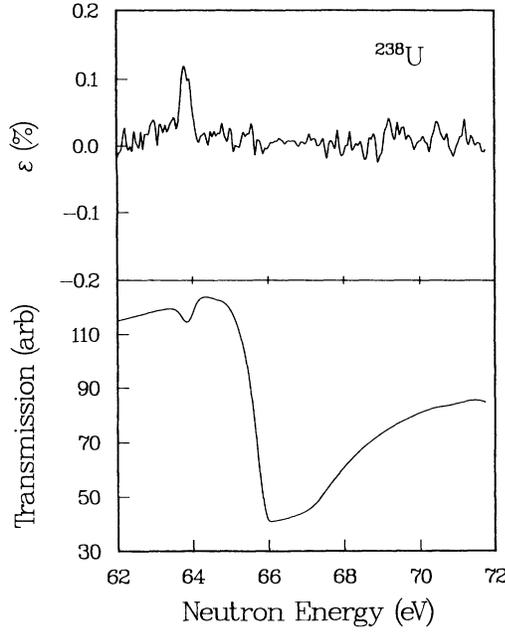
FIG. 1. The lower part shows the neutron transmission in the vicinity of the 63.5-eV resonance. In the upper half the experimental asymmetry $\varepsilon = -(N^+ - N^-)/(N^+ + N^-)$ is shown, where N^+ and N^- are the counts for the two helicity states.

nance is close to a large s-wave resonance, and the large asymmetry clearly indicates parity violation for the 63.5-eV resonance. One could simply take the measured value of ε and extract P directly. However, Doppler broadening has been neglected, as have other finite resolution

effects, and background corrections may be important. Therefore, we devised an analysis method which fits the transmission spectra of both helicities simultaneously.

Doppler broadening effects are important at these energies [37]. Since the p-wave partial neutron width Γ_p^n is proportional to $E^{3/2}$ and λ^2 is proportional to E^{-1}, σ_p can be written $\sigma_p = \beta E^{1/2}/[P]^2$, with β a constant and $\sigma_{\max} = 4\beta(E_p)^{1/2}/\Gamma_p^2$. Let v (V) be the neutron (target) velocity and m (M) the neutron (target) mass. If the target nuclei obey the Boltzmann distribution

$$F(V) = (M/2\pi k_B T)^{3/2}\exp(-MV^2/2k_B T) , \qquad (11)$$

where k_B is Boltzmann's constant and T the temperature, then the Doppler-broadened cross section is

$$\sigma_{\mathrm{eff}}(E_n) = \int \sigma_p(v, V)F(V)dV . \qquad (12)$$

Two convenient dimensionless parameters are $B^2 = (2E_p/\Gamma_p)^2$ and $C = (E_p A/k_B T)^{1/2}$, with A the atomic number of the target nucleus. Since it is desirable to fit the transmission spectra directly, we write the velocity v in terms of constants related to the time-of-flight (TOF) spectrum

$$v/v_0 = [L/(K - K_s)d]/[L/(K_0 - K_s)D]$$
$$= [K_0 - K_s]/[K - K_s] , \qquad (13)$$

where v_0 is the neutron velocity at the resonance energy, L the length of the flight path, D the TOF bin width, K the TOF channel number, K_0 the channel number of the resonance peak, and K_s the time-zero TOF channel number. In terms of these parameters the effective cross section can be written

$$\sigma_{\mathrm{eff}}(K) = \sigma'_{\max}\int_{-\infty}^{+\infty} e^{-u^2}\frac{|(K_0 - K_s/(K - K_s) - u/C|}{1 + B^2\{1 - [(K_0 - K_s)/(K - K_s) - u/C]^2\}^2}du , \qquad (14)$$

where $\sigma'_{\max} = \sigma_{\max}/\pi^{1/2}$. Since we have not explicitly considered the effects of finite beam resolution, etc., some of the fit parameters cannot be interpreted literally. However, this ansatz does provide a convenient phenomenological fitting procedure.

We use the following form for the transmission yield at the detector:

$$N^{\pm} = C^{\pm}\exp[-n\sigma'_{\max}\varphi(1 \pm f_n p)]$$

$$= \frac{N'(1 \pm \alpha)}{K - K_s}\left[1 + \sum_{i=1}^{5}\alpha_i\left[\frac{K - (K_b + K_e)/2}{1000}\right]^i\right]\exp[-n\sigma'_{\max}\varphi(1 \pm f_n p)] , \qquad (15)$$

where $C^{\pm}$ is the flux, $(\sigma'_{\max}\varphi)$ the Doppler broadened p-wave resonance line shape, N' the normalization factor, K the TOF channel number, K_s the effective zero channel determined from the energy calibration, α the beam asymmetry in the two helicity states, and $[K_b, K_e]$ the range of channels under consideration. The polynomial in the square brackets accounts extremely well for effects which change slowly with energy, and provides an adequate description of the background even when the cross section is changing rapidly with energy. Thus this polynomial background simulates the s-wave background well for all of the resonances in ^{238}U. The adjustable parame-

ters for the yield are α_{1-5}, the flux parameters; N', the normalization; K_0, the channel number for resonance peak; $B^2 = (2E_p/\Gamma_p)^2$, the resonance parameter; $C = (E_p A/k_B T)^{1/2}$, the Doppler broadening parameter; $\sigma'_{\max}$, the peak resonance cross section, α, the beam asymmetry; and $f_n P$, the neutron polarization times the parity-violating asymmetry.

Consider the effect of a beam-related background. Assume that the yield is

$$N = C\{\exp[-nt\sigma'_{\max}\phi(1 \pm f_n P)] + B\} , \qquad (16)$$

with the parameter B the ratio of the background to the

true neutron signal. For the ^{238}U target, the product $nt=0.12$/b, $\sigma_{max}\approx 5$ b, and $\phi\approx 0.1$ for a typical p-wave resonance, which yields a value for the product $nt\sigma'_{max}\approx 0.04$. Therefore one can expand the exponential and keep only first order terms, obtaining

$$N=C(1+B)\{1-nt\sigma'_{max}\phi(1+f_nP)/(1+B)\}$$

$$=C'\exp[-nt\sigma''_{max}\phi(1+f_nP)]\,, \qquad (17)$$

with $C'=C(1+B)$ and $\sigma''_{max}=\sigma'_{max}/(1+B)$. To first order the background affects only the overall normalization and the peak cross section, and not the value of P. In practice, as we describe in Sec. V, this analysis method works extremely well.

IV. EXPERIMENTAL DATA

The ^{238}U production data were taken with a TOF bin width of 200 ns. In principle this covers the neutron energy range of 6–1000 eV. In practice the combination of poorer energy resolution and low detector efficiency at higher energies limited the analysis to data below 300 eV. The neutron transmission yields were measured for both helicities. As described above, the neutron yields are sorted by helicity states and according to whether the beam stability (as determined by the fluctuations in the monitor counts) is acceptable or not, i.e., whether the data are accepted ("good") or rejected ("bad").

The production runs were carefully inspected before being accepted for final analysis. In the final analysis we included 123 "good" runs with the proton polarization antiparallel to the field and 58 "good" runs with the proton polarization parallel to the field.

The transmission asymmetry ε, the line shape, and the timing also were inspected. No significant false asymmetry was observed in the ε plots, the resonance line shapes appeared consistent throughout, and the timing was very stable except for a few runs. There is background in the data, as is evident from the shape of the strong s-wave resonances (see Fig. 1). These resonances should be black, but have background arising from γ rays in the neutron beam and scintillator afterglow. However, as noted in Sec. III, to first order such a background does not affect the determination of the parity violating asymmetry.

The relative neutron polarization for each run was determined from the NMR signal measured at the beginning of each run. As discussed in Ref. [34], the NMR signal A_{NMR} is proportional to the proton polarization and the neutron polarization f_n is related to the NMR signal by $f_n=\tanh(\text{const}\times A_{NMR})$. After the combination f_nP was determined for each run, the value of f_n was used to obtain the parity violation P.

The neutron time of flight $TOF=7.23\times 10^{-5}L/(E_n)^{1/2}$, where TOF is in seconds, L in meters, and E_n in eV. The transmission spectrum for ^{238}U in the energy range of interest is shown in Fig. 2. The known resonances in ^{238}U up to 280 eV are listed in Table 1 [38]. The product $g\Gamma_n$ is listed for each resonance, where g is the statistical weight factor. In general the spins of the p-wave resonances are not known. An energy calibration

TABLE I. ^{238}U resonance parameters.

E_n (eV)	l	$g\Gamma_n$ (meV)	E_n (eV)	l	$g\Gamma_n$ (meV)
6.671	0	1.49	145.62	0	0.90
10.237	1	0.001 65	152.42	1	0.039
11.309	1	0.000 39	158.98	1	0.011
19.529	1	0.001 3	160.85	1	0.005
20.872	0	10.2	165.26	0	3.4
36.680	0	33.8	173.18	1	0.033
45.17	1	0.000 90	189.67	0	174.0
49.62	1	0.000 9	194.80	(1)	0.04
57.9	1	0.000 50	200.69	1	0.064
63.52	1	0.005 8	203.11	1	0.037
66.02	0	24.4	208.49	0	49.9
80.73	0	1.9	214.88	1	0.050
83.68	1	0.006 9	218.36	1	0.032
89.24	1	0.085	224.60	1	0.02
93.14	1	0.006	237.30	0	28.0
98.20	1	0.004 8	242.73	1	0.18
102.54	0	70	253.90	1	0.110
111.25	1	0.008 5	257.16	1	0.02
116.87	0	25.2	263.94	1	0.25
121.61	1	0.006	273.62	0	25.0
124.97	1	0.019	275.19	1	0.16
133.30	(1)	0.013	282.46	1	0.10

was obtained by performing a least square fit to the energies and channel numbers of well-identified resonances. (Note that for the thick target used in this experiment the strong s-wave resonances should be black, but due to background effects are not. In any case with a thick target it is difficult to determine precisely the channel number corresponding to the resonance energy for the large s-wave resonances. We therefore used the strongest p-wave resonances to determine the calibration.)

The expression for the TOF can be rewritten in terms of channels: $K(E)^{1/2}=K_s(E)^{1/2}+A$, with K the TOF channel, K_s the zero-TOF channel, and $A=(7.23\times 10^{-5})L/(200\times 10^{-9})$, where 200×10^{-9} s is the TOF bin width. From the least square fit (to the strong p-wave resonances) the best values of K_s and A
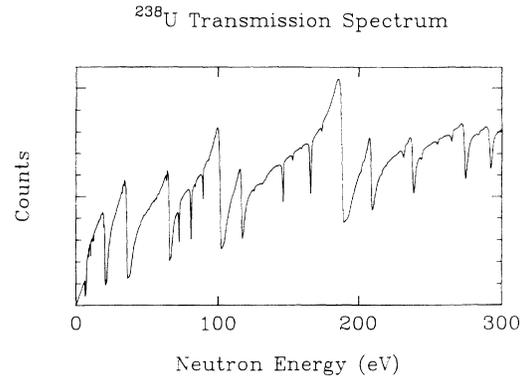
FIG. 2. The ^{238}U transmission spectrum up to $E_n=300$ eV. The data are the sum of all runs used in the final analysis.

were determined. The values of L and K_s are $L=56.51$ m and $K_s=-18.57$. With this calibration the resonances in the experimental spectrum can be identified. The average difference between the calculated and tabulated resonance energies is less than 0.3 eV. We observe all of the s-wave resonances and 29 of the 31 p-wave resonances listed [38] from 6 to 282 eV. More recent evaluations [39,40] have substantially changed the level scheme; however, none of the 16 resonances which we studied in detail had their angular momentum assignment changed. The set of 16 represents the strongest and most well isolated of the p-wave resonances. There are a number of contaminant peaks in the spectrum; all of these have been identified.

V. DATA REDUCTION

Runs with the same proton polarization direction were analyzed together. For each proton polarization direction all of the "good" spectra were combined to form a summed spectrum. We first fit the summed spectrum to determine the line-shape parameters which could be assumed constant from run to run, and then fit the individual runs to obtain a parity-violating asymmetry P for each run. During the latter procedure only a few parameters were adjusted.

The summed spectra were fit as follows: the zero-TOF channel was taken from the calibration, the parameters α_{1-5}, α, and $f_n P$ were initially set equal to zero, K_0 was estimated by inspection, C was calculated at $T=300$ K, and N' and σ'_{max} were set to a nonzero value. The parameter $B^2=(2E_p/\Gamma_p)^2$ can be conveniently expressed in terms of channel numbers. Energy and channel number are related by $\Delta E/E_0=-2\Delta K/K_0$, with E_0 the resonance energy and K_0 the corresponding channel number, and ΔE and ΔK the width in energy and channel numbers. Assuming $\Delta E\approx\Gamma$, this gives $B^2=(K_0/\Delta K)^2$. Therefore B^2 can be conveniently estimated directly from the transmission spectrum.

The first step in the fitting procedure is to free only N' in order to obtain an approximate normalization. Since

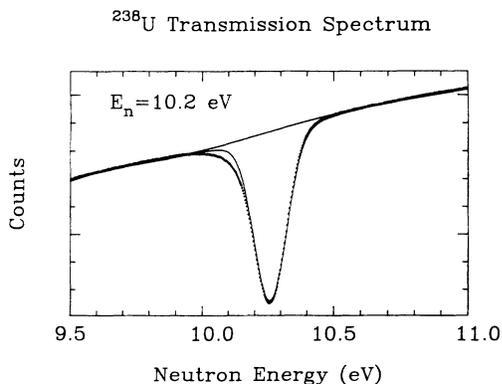### ^{238}U Transmission Spectrum

FIG. 3. The summed transmission spectrum in the vicinity of the 10.2-eV resonance. The solid curves represent fits to the background and to the resonance. As described in Sec. V, the resonance parameters were obtained from the summed spectrum, and then with these resonance parameters held fixed, the longitudinal asymmetries P were obtained for each run.

the dependence on N' is linear, an approximate value for N' is obtained rapidly. Then the parameters α_i are freed one or two at a time, as well as N'. Then K_0 and σ'_{max} are freed in order to obtain the correct peak position and depth. Then the parameter B^2 and C are freed—these are difficult to fit because they may be strongly correlated. Then all remaining parameters are freed. A sample fit is shown in Fig. 3.

The major problem in practice was that some solutions led to unphysical behavior for the flux. We impose the condition that the calculated flux must vary smoothly through the resonance region. To aid in this process, certain regions of the spectrum (corresponding to neighboring resonances which strongly distort the flux shape) were omitted from the analysis. We also studied in detail the effects of changing the size of the region analyzed. To test the reliability of the analysis procedure, two independent analyses were performed for selected resonances. The results are always consistent within the errors quoted.

Once the line-shape parameters $(\alpha_{1-5}$, B^2, C, and $\sigma'_{max})$ were obtained from the summed spectra, the individual runs were fit with only N', K_0, α, and $f_n P$ allowed to vary. The fit usually converged after several iterations.

For each individual run k a value of $(f_n P)_k$ was extracted. Since the polarization f_n is known for each run, a value of P_k can be calculated for each run k. The average parity-violating asymmetry $\bar{P}$ is the weighted average of the individual P_k values. The weighting factors are the errors assigned to each value of $f_n P$ by the fitting program. These errors should be reliable measures of the relative uncertainty in each P_k value, but may not be appropriate for the overall error in $\bar{P}$. An alternative method is to determine the error in $\bar{P}$ from the P_k distribution. The P_k values are histogrammed and the overall error δ determined from $\delta=\sigma/N^{1/2}$, where N is the number of runs and σ^2 is the variance of the P_k data set:

$$\sigma^2=(N-1)^{-1}\sum_{k=1}^{N}(P_k-\bar{P}_{hist})^2 , \qquad (18)$$

where $\bar{P}_{hist}=(\sum_k P_k)/N$. A typical histogram is shown in Fig. 4. In the absence of variations in beam polariza-
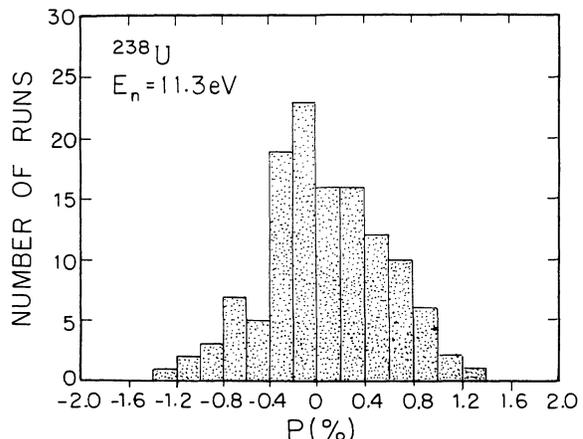
FIG. 4. Histogram of the P values for 123 runs at the 11.3-eV resonance. $\bar{P}=0.67\pm0.37\%$, where the error $\delta=\sigma/N^{1/2}$.

tion and intensity, the observed error σ should be determined by the statistics of a single run. Since δ is determined directly from the distribution, it should include all sources of error and be the most robust way to determine the overall error. The fact that the histograms for all resonances are consistent with a Gaussian is encouraging. The error in $\bar{P}$ also can be estimated from the counting statistics, that is from σ_k. In most cases the error estimated in this way is smaller than the value of δ. This does not necessarily imply that there are nonstatistical errors. For the multiscaler data taken in another experiment [18] the two errors were approximately equal. The discrepancy probably arises from an incorrect conversion factor from transient digitizer voltage to neutron counts, with the error in the transient digitizer data underestimated.

One possible flaw in this procedure for determining the error in $\bar{P}$ is that the underlying distribution is assumed Gaussian in order to obtain $\delta = \sigma / N^{1/2}$. We therefore analyzed a number of the P_k histograms using a statistical approach which makes no assumptions about the underlying distribution. In the Bootstrap method [41] one takes the experimental set of N numbers $\{P_k\}$ and samples with replacement to obtain a new set of N P_k values. Note that a given entry may occur more than once or not at all. From this new distribution the value of $\bar{P}$ is determined. Then the whole procedure is repeated many times. The result is a distribution of $\bar{P}$ values. A nuclear physics application of this technique is described by Shriner *et al.* [42]. For comparison purposes one can use the central 68% of this distribution and interpret the (half) width of this range as the equivalent of the variance for a normal distribution. For the ^{238}U data, the bootstrap distributions were symmetric and the values of δ were consistent with those obtained directly from the histograms and dividing by $N^{1/2}$. Therefore the distribution of the individual parity violations is consistent with no nonstatistical errors.

One additional correction involves the spin flipper [35]. In the above analysis the spin preserving and flipping efficiencies were implicitly assumed to be 100%. The spin-preserving efficiency s (same) is essentially 100% over the energy range of interest, while the spin-flipping efficiency r (reversed) is almost 100% at low energies, but oscillates at higher energies. Assume that the neutrons emerge from the spin filter with polarization f_n. After passing through the spin flipper the neutron polarization is rf_n if the transverse field is on, and sf_n if the transverse field is off. If the initial beam has negative helicity, then

$$\sigma^+ = \sigma_p(1 + rf_n P) \text{ and } \sigma^- = \sigma_p(1 - sf_n P) , \quad (19)$$

where σ^+ and σ^- are the resonance cross sections for the different helicities, and P is the true parity-violating asymmetry. The parity-violating asymmetry obtained from the fitting program is

$$f_n P_{\text{code}} = (\sigma^+ - \sigma^-)/(\sigma^+ + \sigma^-) = f_n P[(r+s)/2] . \quad (20)$$

If the average spin-flipper efficiency is defined as $F_{\text{eff}} = (r+s)/2$, then the true parity-violation P is

TABLE II. Spin-flipper efficiencies, longitudinal analyzing powers, and relative significance of parity-violating asymmetries for p-wave neutron resonances in ^{238}U.

E_n (eV)	F_{eff}	P_i (%)	$|P_i|/\delta_i$
10.2	0.98	-0.16 ± 0.08	2.0
11.3	0.99	0.67 ± 0.37	1.8
45.2	0.93	-1.31 ± 2.10	
63.5	0.88	2.63 ± 0.40	6.6
83.7	0.91	1.96 ± 0.86	2.3
89.2	0.93	-0.24 ± 0.11	2.1
93.1	0.93	-0.03 ± 2.30	
98.0	0.95	-2.18 ± 1.30	1.7
125.0	0.99	1.08 ± 0.86	1.2
152.4	1.00	-0.14 ± 0.56	
158.9	1.00	-0.36 ± 1.37	
173.1	0.99	1.04 ± 0.71	1.5
242.7	0.92	-0.61 ± 0.63	
253.9	0.91	-0.16 ± 0.65	
263.9	0.90	-0.01 ± 0.42	
282.4	0.87	0.41 ± 1.40	

$P_{\text{code}} / F_{\text{eff}}$. This correction has been included in the final values quoted for the parity violation P. The parity violations are listed in Table II and plotted in Fig. 5. (There are a few changes from the preliminary results reported in Bowman *et al.* [19] which arise from reanalysis of the data. The resonance reported at 57.9 eV is obscured by contaminant ^{235}U s-wave resonances which prevent a reliable analysis. This resonance is no longer included in the set of analyzed resonances.)

In addition to the evidence against nonstatistical errors discused above—no false asymmetries in the ε plots and no anomalous shapes in the histograms of the parity violations—we also analyzed some contaminant s-wave resonances. The s-wave resonances are not expected to show parity violation. We analyzed five s-wave resonances which are due to the contaminants ^{235}U, ^{139}La, and ^{65}Cu. The results are listed in Table III. Since the resonances are intrinsically strong, but the isotopes occur only in trace amounts, these contaminant s-wave resonances are comparable in size to the p-wave resonances being analyzed in ^{238}U. None of these five s-wave resonances showed a statistically significant parity violation.

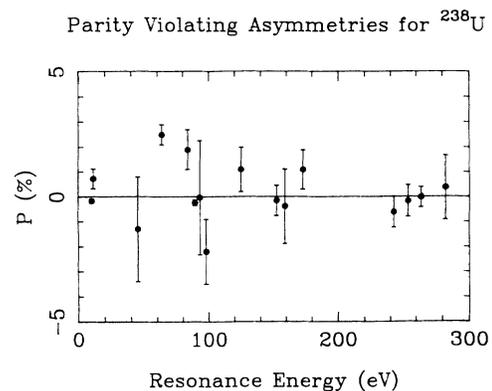Parity Violating Asymmetries for ^{238}U

FIG. 5. The parity-violating longitudinal asymmetries for sixteen resonances in ^{238}U.

TABLE III. Longitudinal analyzing powers for s-wave neutron resonances in ^{235}U, ^{139}La, and ^{65}Cu.

E_n (eV)	P_i (%)
8.97 (^{235}U)	0.05±0.16
11.67 (^{235}U)	−0.18±0.33
12.43 (^{235}U)	−0.22±0.16
72.17 (^{139}La)	−0.02±0.04
230.0 (^{65}Cu)	0.01±0.33

VI. ANALYSIS

The approach described in Sec. I has two major limitations. The two-level approximation is not valid, and in general the spins of the p-wave resonances are unknown. We first consider these issues and then extract a PNC matrix element.

In the two-level approximation the parity violation is

$$P = [2V/(E_s - E_p)][\Gamma_s^n/\Gamma_p^n]^{1/2} , \qquad (21)$$

where the neutron widths are evaluated at the resonance energy E_p. The expression for P can be generalized to include the effects all of the s-wave resonances on a given p-wave resonance. If the s-wave resonances are labeled by j and the p-wave resonances by i, then

$$P_i = \sum_j A_{ij} V_{ij} , \qquad (22)$$

where

$$A_{ij} = [2/(E_{sj} - E_{pi})][\Gamma_{sj}^n/\Gamma_{pi}^n]^{1/2} . \qquad (23)$$

Since the energies and neutron widths are known for all of the s-wave resonances, and the energies and the product $(2J+1)\Gamma^n$ are known for the p-wave resonances, the A_{ij}'s can be calculated. In determining A_{ij}, s-wave resonances up to 500 eV were included. In practice the contributions from a few neighboring levels were much larger than the contributions from the other resonances explicitly included.

The PNC matrix elements V_{ij} are assumed to be Gaussian distributed random variables with mean zero and variance M^2: $\langle V_{ij} \rangle = 0$ and $\langle V_{ij}^2 \rangle = M^2$. If Γ_s^n, Γ_p^n, and the energy spacings are uncorrelated with the V_{ij}, the observable P_i is a Gaussian distributed random variable. The sum of Gaussian random variables is also a Gaussian random variable [43]. The ensemble averages of P_i and P_i^2 are then

$$\langle P_i \rangle = \sum_j A_{ij} \langle V_{ij} \rangle = 0 ,$$

$$\langle P_i^2 \rangle = \langle (\sum_j A_{ij} V_{ij})(\sum_{j'} A_{ij'} V_{ij'}) \rangle$$

$$= \sum_j A_{ij}^2 \langle V_{ij}^2 \rangle = A_i^2 M^2 , \qquad (24)$$

where $A_i^2 = \sum_j A_{ij}^2$. Including the experimental uncertainty δ_i leads to a variance $\langle P_i^2 \rangle = A_i^2 M^2 + \delta_i^2$ for the distribution of P_i values. The probability for measuring a parity-violating asymmetry between P_i and $P_i + dP_i$ is

$$F(P_i) dP_i = \frac{1}{(2\pi \langle P_i^2 \rangle)^{1/2}} \exp\left[-\frac{P_i^2}{2\langle P_i^2 \rangle} \right] dP_i$$

$$= \frac{1}{[2\pi(M^2 + \delta_i^2/A_i^2)]^{1/2}} \exp\left[-\frac{(P_i/A_i)^2}{2(M^2 + \delta_i^2/A_i^2)} \right] dP_i/A_i$$

$$= \frac{1}{[2\pi(M^2 + \delta_{Q_i}^2)]^{1/2}} \exp\left[-\frac{Q_i^2}{2(M^2 + \delta_{Q_i}^2)} \right] dQ_i , \qquad (25)$$

where $Q_i = P_i / A_i$ and $\delta_{Q_i} = \delta_i / A_i$. The new variable Q has the property that its mean is zero and its variance M^2: $\langle Q_i \rangle = 0$ and $\langle Q_i^2 \rangle = M^2$. This crucial result implies that if the A_{ij} are known, the value of the root-mean-square matrix element M can be determined directly from the measured values P_i. The values of P, A, and Q are listed in Table IV. The statistical significance P_i/δ_i of the longitudinal analyzing powers are shown in Fig. 6.

The other problem is that the spins of most of the p-wave resonances are unknown. We therefore assume that the angular momentum values of the p-wave resonances are completely unknown, and adopt a statistical approach. The level density in the compound nucleus can be written as

$$\rho = (2J+1)\exp[-(J+1/2)^2/2\sigma^2] , \qquad (26)$$

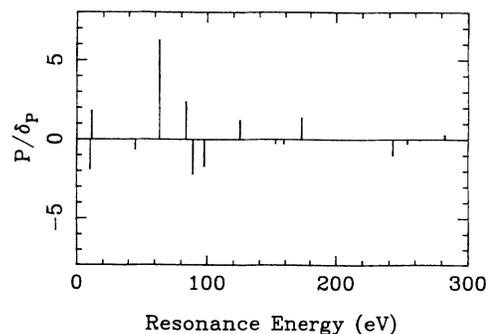Parity Violating Asymmetries for ^{238}U

FIG. 6. Relative significance of parity-violating asymmetries in ^{238}U.

where σ is the spin cutoff parameter, which for ^{238}U has a value of approximately 4.8 [44]. For low spins in ^{239}U it is a good approximation to assume that the CN level density is proportional to $(2J+1)$. We assume a $\frac{1}{3}$ probabili- ty for the p-wave resonances to have $J=\frac{1}{2}$ and a $\frac{2}{3}$ proba- bility to have $J=\frac{3}{2}$. Therefore the probability for a reso- nance to show a parity-violating asymmetry between P_i and P_i+dP_i is

$$F(P_i)dP_i=\left\{\frac{1}{3}\frac{1}{[2\pi(M^2+\delta_{Q_i}^2)]^{1/2}}\exp\left[-\frac{Q_i^2}{2(M^2+\delta_{Q_i}^2)}\right]+\frac{2}{3}\frac{1}{(2\pi\delta_{Q_i}^2)^{1/2}}\exp\left[-\frac{Q_i^2}{2\delta_{Q_i}^2}\right]\right\}.$$ (27)

The likelihood function is the joint probability of all 16 p-wave resonances and can be written as

$$L(M)=N_0\prod_{i=1}^{16}\left\{\frac{1}{3}\frac{1}{[2\pi(M^2+\delta_{Q_i}^2)]^{1/2}}\exp\left[-\frac{Q_i^2}{2(M^2+\delta_{Q_i}^2)}\right]+\frac{2}{3}\frac{1}{(2\pi\delta_{Q_i}^2)^{1/2}}\exp\left[-\frac{Q_i^2}{2\delta_{Q_i}^2}\right]\right\},$$ (28)

where N_0 normalizes the likelihood function as $\int_0^{M_{max}}L(M)dM=1$. We chose $M_{max}=10$ meV for the normalization. The results were insensitive to the value used for the relative number of $J=\frac{1}{2}$ and $\frac{3}{2}$ states.

The likelihood function is shown as a smooth curve in Fig. 7. The most compact region of 68% confidence level is indicated by vertical lines. The most likely value of M is

$$M=0.56^{+0.41}_{-0.20}\text{ meV}.$$ (29)

From the value of M and the s-wave level spacing $D=21.0$ eV [40], the value of the parity-violating spread- ing width is

$$\Gamma^{PV}=2\pi M^2/D=0.9^{+1.9}_{-0.5}\times10^{-7}\text{ eV}.$$ (30)

In the simplest picture, the ratio of the symmetry- breaking strength to the symmetry-conserving strength is given by

$$|\alpha_p|=[\Gamma^{PV}/(2\pi\times10^5\text{ eV})]^{1/2}\approx4^{+3}_{-2}\times10^{-7}.$$ (31)

TABLE IV. Parity violations for p-wave resonances in ^{238}U.

E_n (eV)	P_i (%)	A_i (1/eV)	Q_i (meV)
10.2	−0.16±0.08	24.61	−0.07±0.03
11.3	0.67±0.37	47.13	0.14±0.08
45.2	−1.31±2.10	34.82	−0.38±0.60
63.5	2.63±0.40	34.42	0.76±0.12
83.7	1.96±0.86	13.58	1.44±0.63
89.2	−0.24±0.11	4.70	−0.52±0.24
93.1	−0.03±2.30	24.59	−0.01±0.94
98.0	−2.18±1.30	54.21	−0.40±0.24
125.0	1.08±0.86	10.56	1.02±0.82
152.4	−0.14±0.56	4.38	−0.32±1.29
158.9	−0.36±1.37	8.57	−0.41±1.59
173.1	1.04±0.71	7.80	1.33±0.91
242.7	−0.61±0.63	4.87	−1.26±1.28
253.9	−0.16±0.65	3.25	−0.49±2.00
263.9	−0.01±0.42	2.46	−0.05±1.72
282.4	0.41±1.40	4.95	0.82±2.82

The value for $|\alpha_p|$ is qualitatively reasonable, since one expects that the order of magnitude for α_p should be $G_F m_\pi^2/G_S\sim10^{-7}$, where G_F is the Fermi constant and G_S the strong coupling constant. Jonhson *et al.* [33] dis- cuss the procedure for obtaining α_p from the experimen- tal value of the PNC matrix element M.

VII. SUMMARY

We have obtained values of the CN parity-violating matrix elements free of detailed assumptions about nu- clear spectroscopy. Results for 16 resonances provide the first determination of the variance of the parity-violation matrix element. The value $M=0.56^{+0.41}_{-0.20}$ meV corre- sponds to a spreading width $\Gamma^{PV}=0.9^{+1.9}_{-0.5}\times10^{-7}$ eV. An estimate for the symmetry breaking in the effective NN interaction, $|\alpha_p|\sim4\times10^{-7}$, is obtained from the mea- sured variance M^2.

There remain a number of outstanding issues. We want to measure many parity violations in order to im- prove the precision of the experimental determination of M (or equivalently of Γ^{PV}), to understand the mechanism of the parity-violation process, and to test whether Γ^{PV} depends on mass or energy. Accomplishing these goals would be much easier with an improved experimental system. A new system with a much improved spin filter
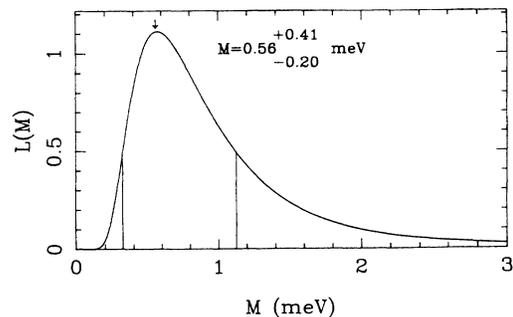

FIG. 7. Likelihood function for the 16 p-wave resonances in ^{238}U. The arrow indicates the value of $M=0.56$ meV, while the vertical lines indicate the range of the 68% confidence level.

and detection system will be available in the near future. The accompanying paper describes an experiment with essentially the same experimental system; these data shed light on the mechanism question. The data for ^{232}Th show a number of resonances with large and statistically significant parity violations, and provide evidence that our purely statistical approach is too simple: the parity violations display sign correlations. Therefore the data must be analyzed with both a constant and a fluctuating term. In practice this only slightly changes the value of the PNC matrix element. This new analysis is discussed in the following paper.

The qualitative goal of these efforts is to map out the weak nuclear potential and to complement and to improve on the experiments and analyses of parity violation in light nuclei. The utilization of the chaotic compound nucleus bypasses many of the complications found in light nuclei, but faces a different set of uncertainties and complications.

[1] E. G. Adelberger and W. C. Haxton, Annu. Rev. Nucl. Part. Sci. 35, 501 (1988).
[2] Yu. G. Abov. P. A. Krupchitsky, and Yu. A. Orlatovsky, Phys. Lett. 12, 25 (1964).
[3] E. Warming, F. Stecher-Rasmussen, W. Ratynski, and J. Kopecky, Phys. Lett. 25B, 200 (1967).
[4] Yu. G. Abov, P. A. Krupchitsky, M. I. Bulgakov, O. N. Ermakov, and I. L. Karpikhin, Phys. Lett. 27B, 16 (1968).
[5] E. Warming, Phys. Lett. 29B, 564 (1969).
[6] Y. G. Abov, M. M. Danilov, O. N. Ermakov, I. L. Karpikhin, V. K. Rissukhin, and A. M. Skornyakov, Yad. Fiz. 16, 1218 (1972) [Sov. J. Nucl. Phys. 16, 670 (1973)].
[7] P. A. Krupchitsky, Fundamental Research with Polarized Slow Neutrons (Springer Verlag, Berlin, 1987).
[8] F. C. Michel, Phys. Rev. 133, B329 (1964).
[9] L. Stodolsky, Phys. Lett. 50B, 352 (1974).
[10] M. Forte, B. R. Heckel, N. F. Ramsey, K. Green, G. L. Greene, J. Byrne, and J. M. Pendlebury, Phys. Rev. Lett. 45, 2088 (1980).
[11] B. Heckel et al., Phys. Lett. 119B, 298 (1982).
[12] O. P. Sushkov and V. V. Flambaum, Pis'ma Zh. Eksp. Teor. Fiz. 32, 377 (1980) [JETP Lett. 32, 352 (1980)].
[13] O. P. Sushkov and V. V. Flambaum, Usp. Fiz. Nauk. 136, 3 (1982) [Sov. Phys. Usp. 25, 1 (1982)].
[14] V. P. Alfimenkov, S. B. Borzakov, Vo Van Thuan, Yu. D. Mareev, L. B. Pikelner, A. S. Khrykin, and E. I. Sharapov, Nucl. Phys. A398, 93 (1983).
[15] S. A. Biryukov et al., Yad. Fiz. 45, 1511 (1987) [Sov. J. Nucl. Phys. 45, 937 (1987)].
[16] Y. Masuda, T. Adachi, A. Masaike, and K. Morimoto, Nucl. Phys. A504, 269 (1989).
[17] C. D. Bowman, J. D. Bowman, and V. W. Yuan, Phys. Rev. C 39, 1721 (1989).
[18] V. W. Yuan et al., Phys. Rev. C 44, 2187 (1991).
[19] J. D. Bowman et al., Phys. Rev. Lett. 65, 1721 (1990).
[20] C. M. Frankle et al., Phys. Rev. Lett. 67, 564 (1991).
[21] C. M. Frankle et al., Phys. Rev. C 46, 778 (1992), the following paper.
[22] E. G. Adelberger, P. Hoodbhoy, and B. A. Brown, Phys. Rev. 30, 456 (1984).
[23] V. E. Bunakov and V. P. Gudkov, Z. Phys. A 303, 285 (1981).
[24] V. P. Alfimenkov, Usp. Fiz. Nauk 144, 361 (1984) [Sov. Phys. Usp. 27, 11 (1984)].

[25] J. R. Vanhoy, E. G. Bilpuch, J. F. Shriner, Jr., and G. E. Mitchell, Z. Phys. A 331, 1 (1988).
[26] C. R. Gould, D. G. Haase, N. R. Roberson, H. Postma, and J. D. Bowman, Int. J. Mod. Phys. A5, 2181 (1990).
[27] V. E. Bunakov and V. P. Gudkov, Nucl. Phys. A401, 93 (1983).
[28] B. Desplanques, J. Phys. Colloq. 45, 55 (1984).
[29] H. A. Weidenmüller, in Fundamental Symmetries in Nuclei and Particles, edited by H. Henrikson and P. Vogel (World Scientific, Singapore, 1989), p. 30.
[30] O. Bohigas and H. A. Weidenmüller, Annu. Rev. Nucl. Part. Sci. 38, 421 (1988).
[31] J. B. French, V. K. B. Kota, A. Pandey, and S. Tomsovic, Ann. Phys. (N.Y.) 181, 198 (1988).
[32] J. B. French, A. Pandey, and J. Smith, in Tests of Time Reversal Invariance in Neutron Physics, edited by N. R. Roberson, C. R. Gould, and J. D. Bowman (World Scientific, Singapore, 1987), p. 80.
[33] M. B. Johnson, J. D. Bowman, and S. H. Yoo, Phys. Rev. Lett. 67, 310 (1991).
[34] N. R. Roberson et al., Nucl. Instrum. Methods (to be published).
[35] J. D. Bowman and W. B. Tippens, Nucl. Instrum. Methods (to be published).
[36] J. D. Bowman, J. J. Szymanski, V. W. Yuan, C. D. Bowman, A. Silverman, and X. Zhu, Nucl. Instrum. Methods A297, 183 (1990).
[37] J. E. Lynn, The Theory of Neutron Resonances (Clarendon Press, Oxford, 1968).
[38] S. F. Mughabghab, Neutron Cross Sections (Academic, New York, 1984), Vol. 1, Pt. B.
[39] JENDL-3 data file for ^{238}U (Japanese Nuclear Data Committee, 1987), evaluation by T. Nakagawa.
[40] ENDF/B-VI data file for ^{238}U (National Nuclear Data Center, Upton, NY, 1989), evaluation by D. K. Olsen, R. Macklin, M. C. Moxon, and M. G. Sowerby.
[41] B. Efron, SIAM Rev. 21, 460 (1979).
[42] J. F. Shriner, Jr., G. E. Mitchell, and E. G. Bilpuch, Nucl. Instrum. Methods A254, 139 (1987).
[43] W. T. Eadie, D. Drijard, F. E. James, M. Roos, and B. Sadoulet, Statistical Methods in Experimental Physics (North Holland, Amsterdam, 1971).
[44] T. von Egidy, H. H. Schmidt, and A. N. Behkami, Nucl. Phys. A451, 189 (1988).